SUPPLEMENTARY INFORMATION

The human 18S rRNA m^{6}A methyltransferase METTL5 is stabilized by TRMT112

Tran N.V.[1,*], Ernst F.G.M.[2,*], Hawley B.R.[3]; Zorbas C.[2], Ulryck N.[1], Hackert, P.[4], Bohnsack K.E.[4], Bohnsack M.T.[4], Jaffrey S.R.[3], Graille M.[1], and Lafontaine D.L.J.[2]

[1]BIOC, CNRS, Ecole polytechnique, Institut Polytechnique de Paris, F-91128 Palaiseau, France

[2]RNA Molecular Biology, ULB Cancer Research Center (U-CRC), Fonds de la Recherche Scientifique (F.R.S./FNRS), Université Libre de Bruxelles, Charleroi-Gosselies, Belgium
[3]Department of Pharmacology, Weill Medical College, Cornell University, NY 10065, New York, U.S.A.
[4]Department of Molecular Biology, University Medical Center Göttingen, 37073 Göttingen, Germany.

* These authors contributed equally.

Corresponding authors:
The last two authors contributed equally to this work.
Denis L.J. Lafontaine. Tel: +32-2-650-9771. E-mail: denis.lafontaine@ulb.ac.be
Marc Graille. Tel: +33-0-169334890. E-mail: marc.graille@polytechnique.edu

Keywords: ribosome biogenesis, nucleolus, translation, methyltransferase, RNA modification, RNA processing

Running title: The elusive human m^{6}A rRNA methyltransferases identified

SUPPLEMENTARY MATERIALS AND METHODS

Pre-rRNA processing analysis

Total RNA extraction was performed as previously described (1). Denaturing agarose gels were stained with ethidium bromide to visualize the large mature rRNAs and transferred to nylon membranes for northern blot analysis with suitable probes (as described in 1). The sequences of the oligonucleotide probes used are listed in Table S4. The 28S/18S ratios were established from electropherograms (Agilent, Bioanalyzer Kit #5067-1511).

Cloning and expression assays

The gene encoding *Hvo*_1475 (hereafter named *Hvo*Mettl5) was amplified by PCR from *H. volcanii* genomic DNA with oligonucleotides oMG439 and oMG440 (Table S5) and the Phusion High-Fidelity DNA Polymerase (Thermo). The PCR products were cloned into the pET28b vector to generate plasmid pMG825 encoding a C-terminally His_6-tagged version of the full-length *Hvo*Mettl5 protein. Generation of the pET21a-derived pMG564 plasmid encoding untagged *Hvo*Trm112 protein has been described previously (2).

DNA sequences optimized for heterologous expression in *E. coli* were designed to encode either *H. sapiens* METTL5 or *H. sapiens* ZCCHC4, each with a C-terminal His_6-tag. These fragments were obtained by *de novo* synthesis (Integrated DNA Technologies, Belgium) and cloned into pET21a between the *Nde*I and *Not*I sites to yield plasmids pMG832 (METTL5) and pMG837 (ZCCHC4). The pFF6 plasmid (kind gift from Dr. V. Heurgué-Hamard, France) was used to express human TRMT112 in *E. coli* (Table S5; 3).

Heterologous expression and purification of the HvoMettl5-Trm112 complex

The *Hvo*Trm112 protein was co-expressed with the His_6-tagged *Hvo*Mettl5 protein in *E. coli* BL21 (DE3) Gold cells (Agilent technologies) upon co-transformation with pMG825 and pMG564 plasmids (Table S5). Cultures were carried out in 1 L auto-inducible Terrific Broth (ForMedium AIMTB0260) containing ampicillin (100 µg/mL) and kanamycin (50 µg/mL), first for 3 h at 37°C and then overnight at 18°C. The cells were harvested by centrifugation at 4000 rpm for 30 minutes. The pellet was resuspended in 30 mL lysis buffer L_{2000} (2 M NaCl, 50 mM Tris-HCl pH 7.5, 5 mM β-mercaptoethanol, 10 µM $ZnCl_2$, and 10 mM imidazole pH 7.5). This complex was purified as previously described for other *Hvo*Trm112-methyltransferase complexes (2).

Heterologous expression and purification of the human METTL5-TRMT112 complex

The human TRMT112 and METTL5-His_6 proteins were co-expressed in *E. coli* BL21 (DE3) Gold (Agilent technologies) from plasmids pMG832 and pFF6. Large-scale purification was done from 1 L of culture in auto-inducible Terrific Broth (ForMedium AIMTB0260) containing ampicillin and chloramphenicol. The culture was initially incubated at 37°C for 3 h and then at 18°C overnight. The cells were harvested by centrifugation at 4000 rpm for 30 min and the pellets were resuspended in 30 mL lysis buffer L_{200} (200 mM NaCl, 50 mM Tris-HCl pH 7.5, 5 mM β-mercaptoethanol). The cells were lysed by sonication on ice and lysate clearance was performed by centrifugation at 20,000 rpm for 45 min. The supernatant was applied to Ni-NTA resin pre-equilibrated with buffer L_{200}, incubated at 4°C on a rotating wheel for 30 min, followed by three washing steps of 20 mL of L_{200}. The

first one was performed with washing buffer L_{1000} (1 M NaCl, 50 mM Tris-HCl pH 7.5, 5 mM β-mercaptoethanol), the second one with L_{200} and the third one with L_{200} supplemented with 20 mM imidazole pH 7.5. The TRMT112-METTL5 complex was eluted with 10 mL elution buffer (lysis buffer L_{200} supplemented with 400 mM imidazole pH 7.5). The protein sample was then diluted in buffer L_{50} (50 mM NaCl, 50 mM Tris-HCl pH 7.5, 5 mM β-mercaptoethanol) and injected onto a HiTrap Q FF column. The protein complex was eluted with a linear NaCl gradient from 100% of buffer L_{50} to 100% of buffer L_{1000}. Fractions containing the TRMT112-METTL5 complex were collected and concentrated to 5 mL, injected onto a S75-16/60 size-exclusion chromatography column (GE Healthcare), and eluted with lysis buffer L_{200}.

Effect of coexpressing HvoTrm112 or TRMT112 on the solubility of the associated methyltransferases

For expression assays, *E. coli* BL21 (DE3) Gold cells transformed with appropriate plasmids (Table S5) were grown in 5 mL TBAI medium supplemented with the relevant antibiotics in 24-deep-well plates, first at 37°C for 3 h and then at 18°C overnight. As ZCCHC4 is predicted to contain a zinc-finger domain, $ZnCl_2$ was added at 100 µM to the culture medium and at 10 µM to the lysis buffer. Cells were harvested by centrifugation at 2000 rpm and 4°C for 15 minutes and then resuspended in 1.2 mL lysis buffer (200 mM NaCl, 20 mM Tris-HCl pH 7.5, 5 mM β-mercaptoethanol) and frozen at -20C°. Thawed cells were sonicated on ice for 1 min. Ten microliters of total extract (TE) was withdrawn for further analysis by SDS-PAGE and western blotting. Cell debris and insoluble proteins were removed by centrifuging for 30 min at 13000 rpm and 4°C. Ten microliters of supernatant (soluble extract or SE) was withdrawn for further analysis by SDS-PAGE and western blotting.

The human ZCCHC4+/-TRMT112 and METTL5+/-TRMT112 proteins were further subjected to an affinity chromatography purification on 50 µL Ni-NTA resin pre-equilibrated with lysis buffer. After extensive washing with 2 mL lysis buffer, the bound proteins were incubated with 50 µL of elution buffer (200 mM NaCl, 20 mM Tris-HCl pH 7.5, 5 mM β-mercaptoethanol, 400 mM imidazole pH 7) prior to elution. Ten microliters of eluate (E) was withdrawn for further analysis by SDS-PAGE and western blotting.

The TE, SE, and E samples were loaded on an 15% SDS-polyacrylamide gel and transferred to a nitrocellulose membrane for immunoblotting. His-tagged proteins were detected with anti-His_6 antibodies coupled to peroxidase (SIGMA: #A7058 (1:2000 dilution), while human TRMT112 was detected with rabbit polyclonal antibodies raised against purified TRMT112-METTL5 complex (COVALAB) (1:2500 dilution) as primary antibodies and HRP-conjugated anti-rabbit IgG (1:20000 dilution; SIGMA: #A6154) as secondary antibody. Membranes were incubated for 5 min with 1 mL Lumi-light^{PLUS} substrate solution (ROCHE: #12015196001) and detection was done with a Chemidoc BioRad system.

Size Exclusion Chromatography - Multi-Angle Laser Light Scattering (SEC-MALLS)
The samples (100 µL at 1 mg/mL) were injected at a flow rate of 0.75 mL/min onto a Superdex^{TM} 200 Increase 10/300 GL column (GE-Healthcare) and eluted with buffers L_{2000} for the *Hvo*Mettl5-Trm112 complex and buffer L_{200} for the METTL5-TRMT112 complex. Elution was monitored with a UV-Visible spectrophotometer, an RID-20A refractive index detector (Shimadzu), and a MiniDawn TREOS detector (Wyatt Technology). The data were collected and processed with the program ASTRA 6.1 (Wyatt Technology) software. M_w was calculated directly from the absolute light scattering measurements, using a dn/dc value of 0.183.

Immunoprecipitation of complexes containing Flag-tagged proteins from human cells
Expression of 2x Flag-PreScission protease cleavage site-His_6-METTL5 (Flag-METTL5) or the Flag tag alone was induced in stably transfected HEK293 cells by addition of 1 µg/mL tetracyline for 24 h before harvesting. Cells were lysed by sonication in a buffer containing 50 mM Tris-HCl pH 7.8, 150 mM NaCl, 0.5 mM EDTA, 0.1 % Trition-X-100 supplemented with protease. Cell debris were pelleted by centrifugation and the clear lysate was incubated with anti-Flag (M2) magnetic beads for 2 h at 4 °C. After thorough washing steps, complexes were eluted using 250 µg/mL Flag peptide and proteins were precipitated using trichloroacetic acid (TCA). Proteins were separated by SDS-PAGE and transferred to nitrocellulose membrane for western blotting using antibodies (anti-PNO1 – Proteintech (21059-1-AP); anti-ENP1 (4); anti-Flag – Sigma-Aldrich (F3165)).

miCLIP bioinformatic analyses
Initial processing of raw FASTQ files was performed as in the miCLIP protocol (5). Adapters and low-quality nucleotides were first trimmed from paired reads with flexbar v2.5, then de-multiplexed with the pyBarcodeFilter.py script of the pyCRAC suite. The remainder of the random barcode was moved to the headers of the FASTQ reads with an awk script and PCR duplicates were removed with the pyCRAC pyDuplicateRemover.py script. Reads were aligned to hg38 with bwa v0.7.17, using the option "-n 0.06" as recommended in the CTK package.

To call m^6A, C-to-T transitions were extracted and the CIMS pipeline of the CTK package was used. Those within the DRACH consensus were then filtered. The sites identified in each replicate were collapsed and metagenes were generated with MetaPlotR (6). In all cases, the longest GENCODE transcript isoform for each gene was selected. For the genome tracks of the ribosomal RNA gene unit, mapped miCLIP reads containing C-to-T transitions were extracted and plotted with pyGenomeTracks v2.0.

To identify ZCCHC4- or METTL5-dependent m^6A sites, mapped miCLIP reads containing C-to-T transitions were first converted to transcript coordinates (GRCh38.93) of the longest isoform per gene. Coverage of these within sliding windows (80-nt-width bins with a step size of 40 nt) was counted and normalized to the median count across all windows per gene. To prevent downstream biases due to low read coverage, bins with less than 2% of the maximum were filtered out. Bins were then tested for

significantly differential counts between the wild type and each knockout, using the exactTest() function of the edgeR package v3.18.1.

miCLIP sequencing data was deposited at the Gene Expression Omnibus database (https://www.ncbi.nlm.nih.gov/geo/) under accession GSE128699.

SUPPLEMENTARY FIGURES

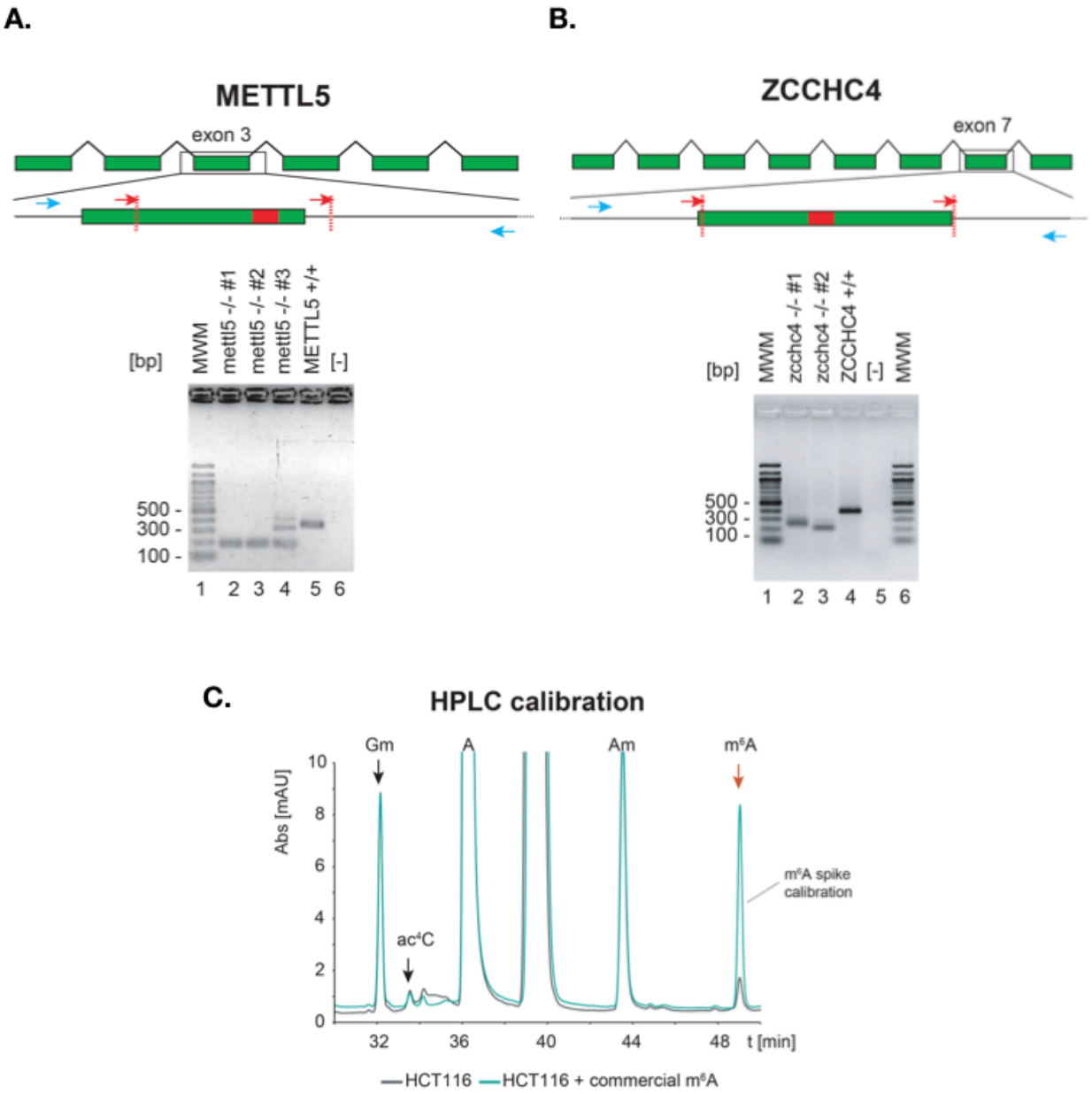

Figure S1: Strategy of METTL5 and ZCCHC4 gene knockout by CRISPR-Cas9 genome editing, diagnostic PCR of the generated cell lines, and m^{6}A calibration of our HPLC system

A-B. METTL5 (A) and ZCCHC4 (B) gene locus structure, highlighting the exon targeted for deletion by CRISPR-Cas9 editing. The region targeted for deletion, containing the methyltransferase domain, is delineated by red dashed lines. Green, exons; red, N6-adenosine methyltransferase signature (123-VIMNPPF-129 for METTL5; 273-MVTDPPF-279 for ZCCHC4); red arrows, CRISPR guides; cyan arrows, oligonucleotides used for diagnostic PCR. All variants generated were sequenced (see Table S3).

C. Calibration of the HPLC system used in this work with a commercial source of m^{6}A nucleoside. Total RNA from HCT116 parental cells digested to nucleosides and spiked with 1 nmol of commercial m^{6}A nucleoside was analyzed by HPLC. Black curve, HCT116 total RNA; green curve, HCT116 total RNA spiked with commercial m^{6}A marker. m^{6}A elutes shortly after 48 min.

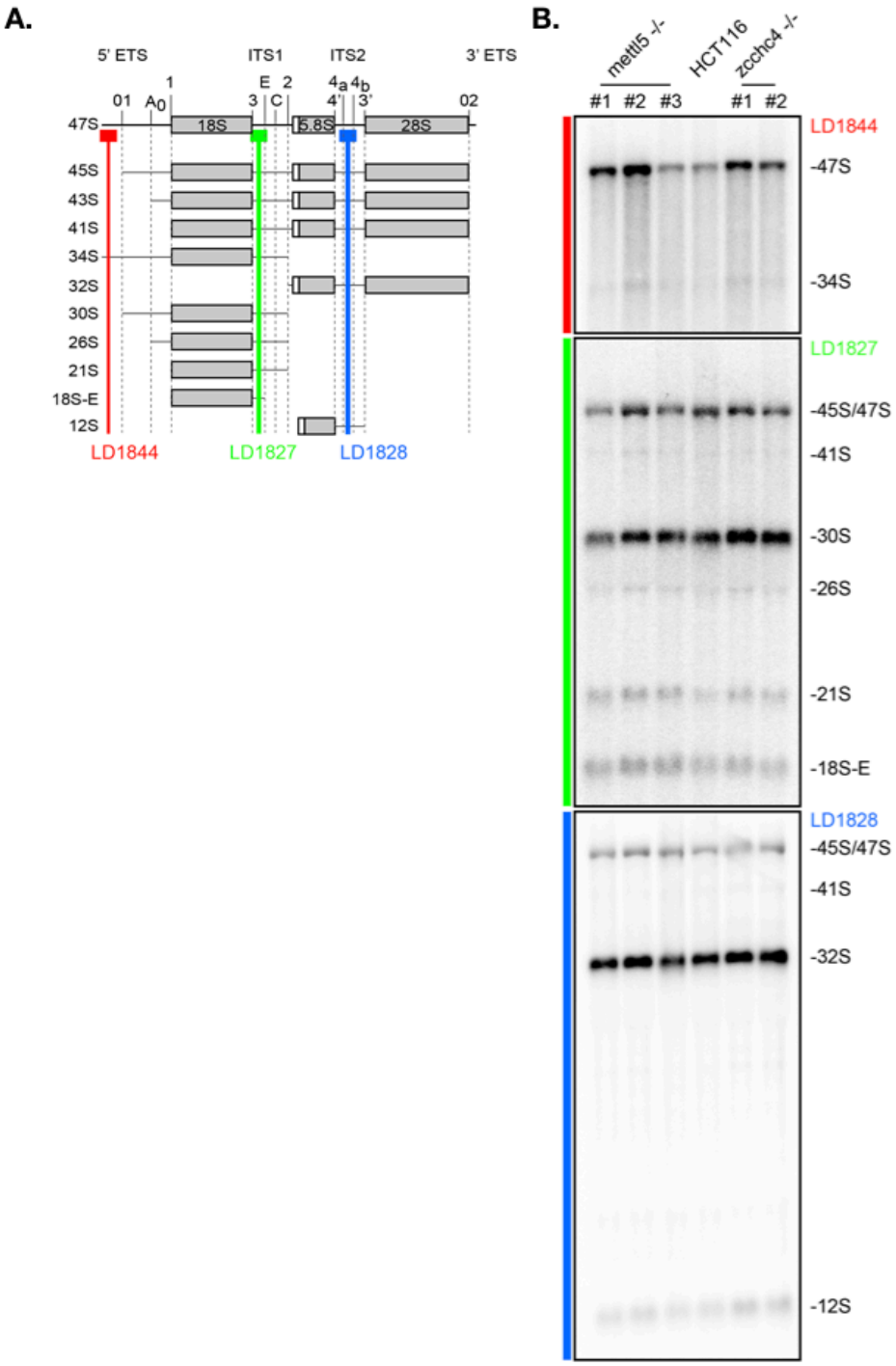

Figure S2: Human METTL5 and ZCCHC4 are not essential to pre-rRNA processing

A. Human pre-rRNA precursors. Three out of four mature rRNAs are produced from a single polycistronic transcript synthesized by RNA polymerase I, the 47S. The mature ends of these rRNAs are produced by extensive processing of the 47S pre-rRNA. The major processing intermediates and northern blot probes used in panel B (LD1844, LD1827, and LD1828) are indicated.

B. Pre-rRNA processing is unaffected in the absence of METTL5 or ZCCHC4. The gel shown in panel B was transferred to nylon and hybridized with probes to detect all major pre-rRNA processing intermediates. The probes used are depicted in panel A. See main text for details.

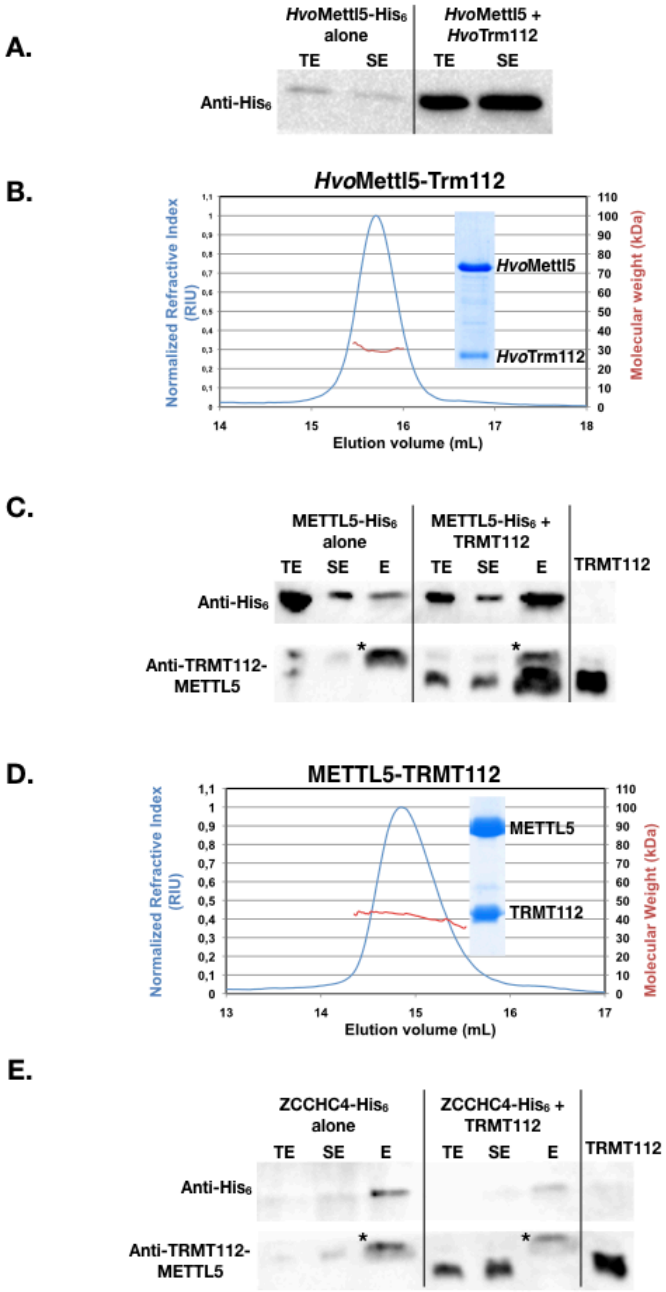

Figure S3: Archaeal and human METTL5 become stable and soluble upon co-expression with TRMT112

A. *Hvo*Trm112 solubilizes *Hvo*Mettl5 upon co-expression in *E. coli*. When *Hvo*Mettl5 and *Hvo*Trm112 are co-expressed in *E. coli*, the stability and solubility of the methyltransferase subunit are improved dramatically. Western blot analysis of total extract (TE) or soluble extract (SE) obtained from cells producing *Hvo*Mettl5-His_6, alone (left) or with *Hvo*Trm112 (right).

B. Chromatogram resulting from SEC-MALLS analysis of the *Hvo*Mettl5-Trm112 complex. A zoom-in centered on the main peak with the refractive index colored in blue (left y-axis) and the distribution of molecular mass calculated from light scattering along this peak colored in red (right y-axis) are shown. SDS-PAGE and Coomassie-staining analysis of the proteins present in the main peak is shown.

C. *Hs*TRMT112 solubilizes *Hs*METTL5 upon co-expression in *E. coli*. Western blot analysis for the detection of METTL5-His_6 (using an anti-His_6 antibody; upper panel), and of TRMT112 (using polyclonal antibodies raised against the purified METTL5-TRMT112 complex; lower panel) in total extract (TE) and soluble extract (SE) from *E. coli*, and in Ni-NTA elution (E) fraction. Note that the antibodies raised against purified METTL5-TRMT112 complex do not react well with human METTL5. The asterisk indicates a non-specific band. As a control, purified human TRMT112 was loaded (right lane).

D. Chromatogram resulting from SEC-MALLS analyses of human METTL5-TRMT112 complex. A zoom-in centered on the main peak with the refractive index colored in blue (left y-axis) and the distribution of molecular mass calculated from light scattering along this peak colored in red (right y-axis) are shown. SDS-PAGE analysis of the Coomassie-stained proteins present in the main peak is shown.

E. Co-expressing TRMT112 with ZCCHC4 has no impact on the stability or solubility of ZCCHC4. Western blot analysis for detection of ZCCHC4-His_6 (using anti-His_6 antibodies, top) and TRMT112 (using antibodies directed against TRMT112-METTL5 human complex, bottom) in total (TE) or soluble (SE) extracts and Ni-NTA elution (E). The asterisk indicates a non-specific band. As a control, purified human TRMT112 was loaded (right lane).

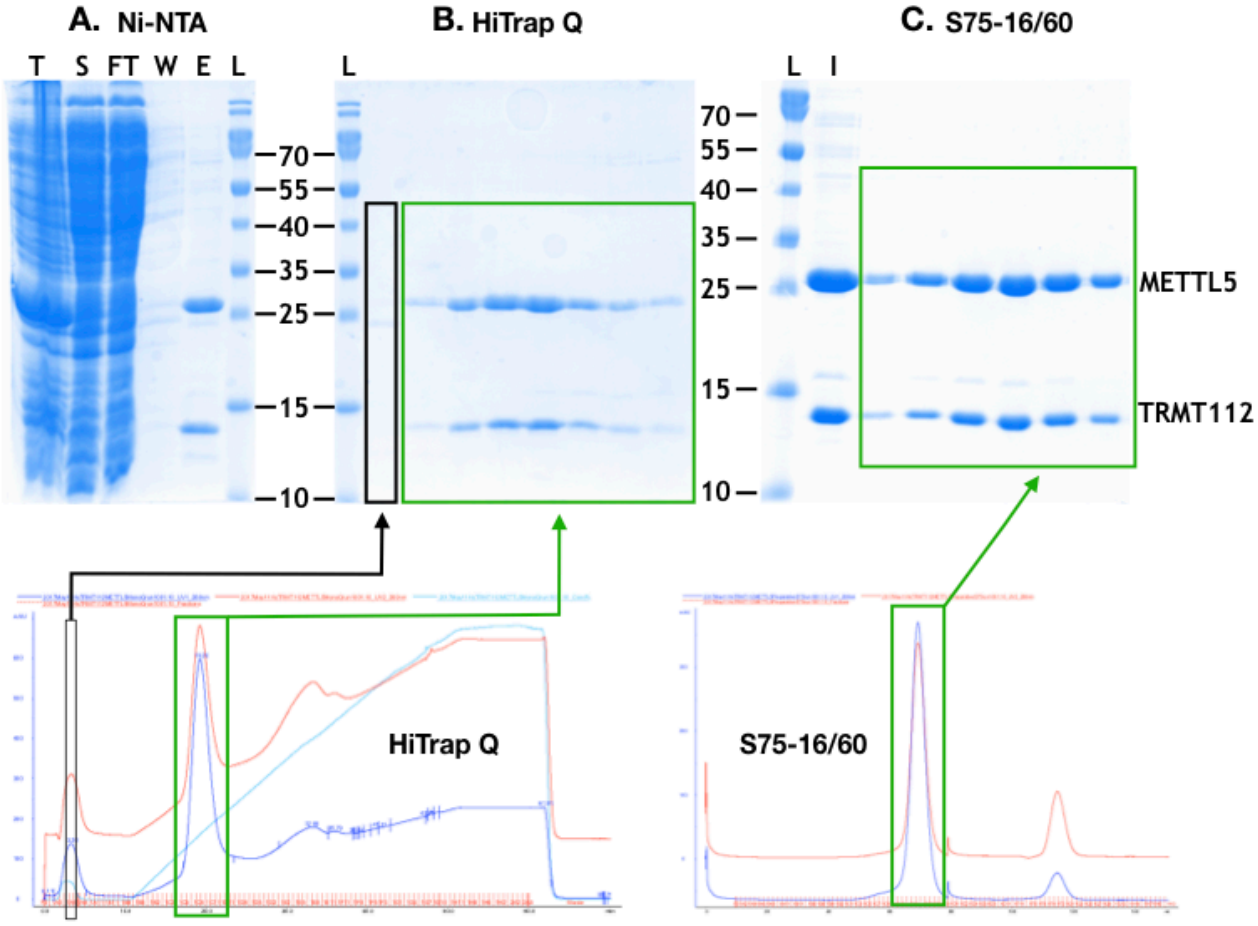

Figure S4: TRMT112 interacts stably and directly with METTL5

Three-step purification procedure of METTL5-TRMT112 complex comprising **A**) affinity chromatography on NiNTA-agarose resin (Ni-NTA), **B**) ion-exchange chromatography (HiTrap Q FF), and **C**) size-exclusion chromatography (S75-16/60). SDS-PAGE analysis of the different fractions from Ni-NTA (T: total extract; S: soluble extract; FT: flow-through; W: wash and E: elution), HiTrap Q and S75-16/60 (I: Injected sample). Chromatograms from HiTrap Q and S75-16/60 steps are show below. Fractions loaded on the SDS-PAGEs are boxed in black (flow-through from HiTrap Q) or green (main peak from each purification step). L: Molecular weight ladder.

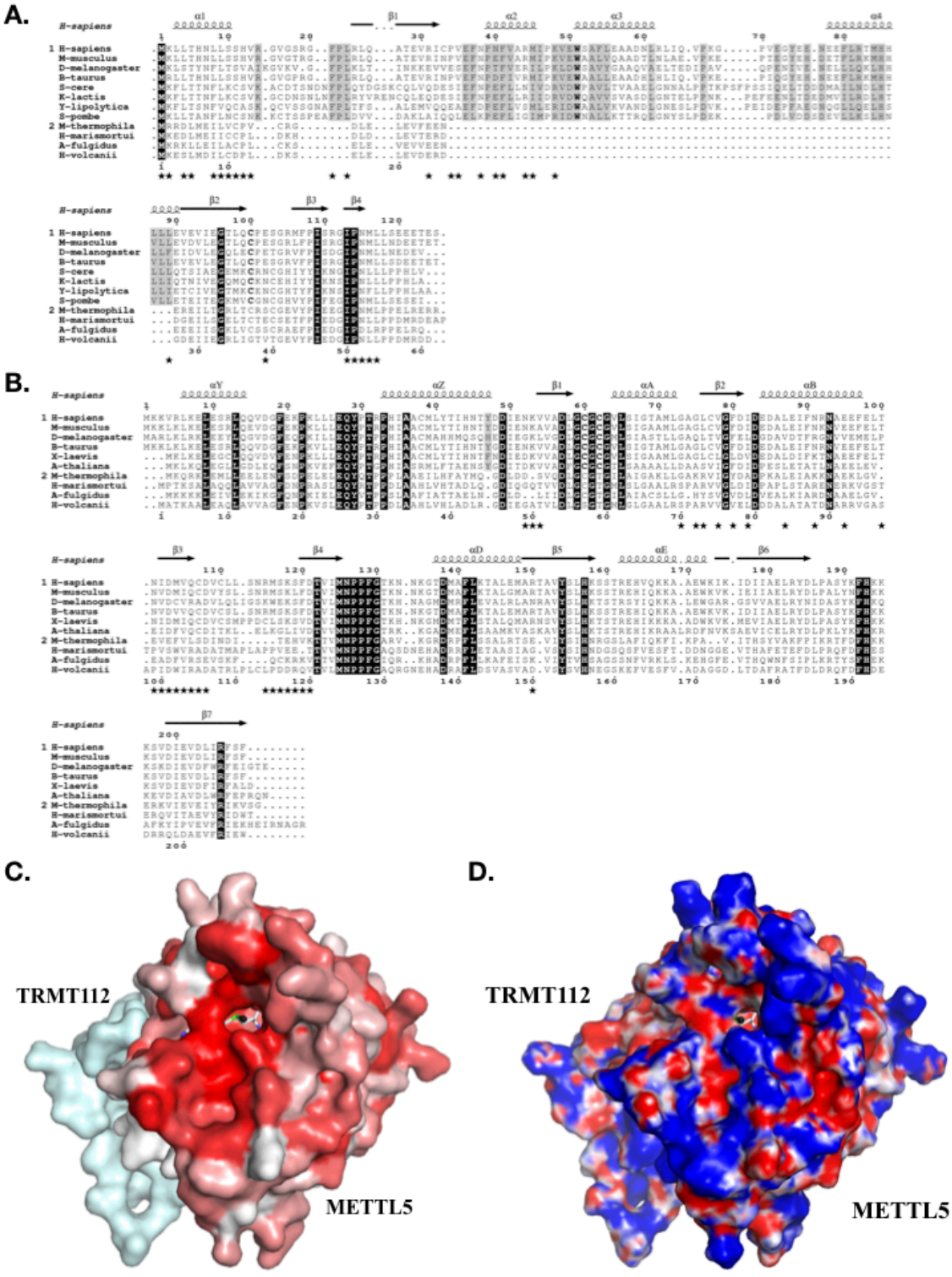

Figure S5: Sequence alignment of Eukaryal and Archaeal TRMT112 and METTL5 proteins and sequence conservation and electrostatic charge distribution on METTL5

A. TRMT112 sequences. Strictly conserved residues appear in white on a black background. Partially conserved amino acids are highlighted with a gray background. Secondary structure elements assigned on the basis of the *H. sapiens* crystal structure established in this work are indicated above the alignment. Black stars, residues involved in complex formation. Display generated using the ENDsript server (7).

B. METTL5 sequences. As in panel B.

C. Mapping of the sequence conservation at the surface of METTL5. Sequence conservation is represented as a gradient of white (no conservation) to red (strict conservation). TRMT112 is shown in light blue. Conservation scores were calculated from an alignment of 29 eukaryotic and archaeal sequences using the ConSurf server (8). The SAM molecule bound to METTL5 active site is shown as sticks and the methyl group to be transferred is shown as a black sphere.
D. Mapping of the electrostatic potential at the surface of human METTL5-TRMT112. Positively charged (5 k_BT/e^-) and negatively charged (–5 k_BT/e^-) regions are colored in blue and red, respectively. The electrostatic potential was calculated using the CHARMM-GUI web server (9,10). SAM and the transferred methyl group are depicted as in panel C.

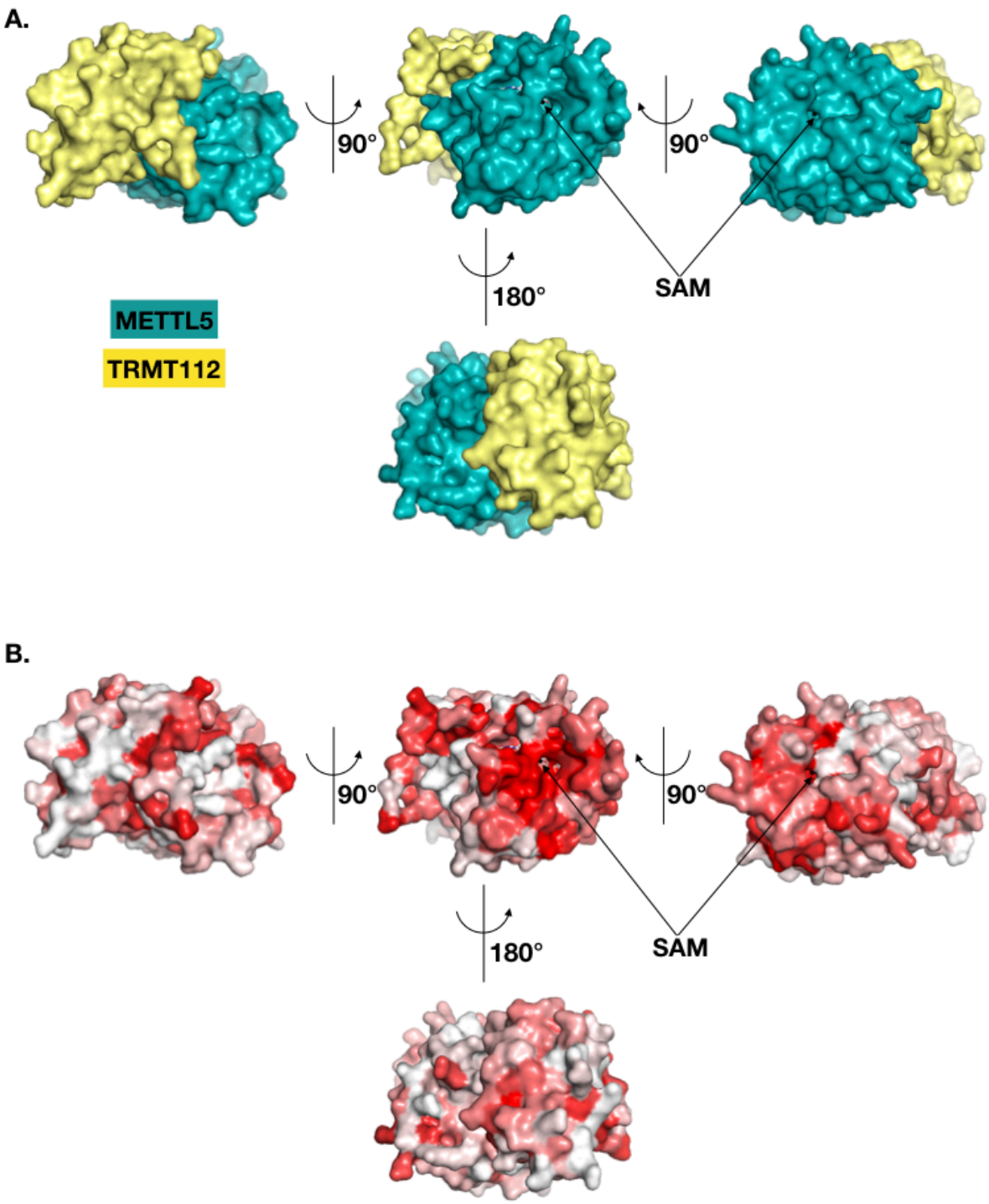

Figure S6: Sequence conservation and electrostatic charge distribution on Eukaryal METTL5-TRMT112 complexes

A. Different views (orientations) of the human METTL5-TRMT112 complex (the SAM binding pocket is highlighted).

B. Sequence conservation at the surface of eukaryotic METTL5-TRMT112 complexes on views shown in panel A (see Figure S5, panel C for details). Sequence conservation was calculated from the multiple alignments of 35 eukaryal METTL5 or TRMT112 sequences from multi-cellular organisms (the same species were used), using as cut off >45% sequence identity. Archaeal sequences were omitted from the alignment as the central domain of TRMT112 is largely missing in archaea.

The surface conservation analysis on TRMT112 reveals the presence of three conserved regions: 1) the area involved in interaction with the methyltransferase subunit (here: METTL5, but it is the same region which is involved in binding the methyltransferases Mtq2/HEMK2, Bud23/WBSCR22, Trm9/ALKHB8, and Trm11/TRMT11, see 11), 2) a small region located close to the putative active site of METTL5 at the tip of the zinc-binding domain (interestingly, in the context of Mtq2-Trm112 and Trm11-Trm112 complexes from *S. cerevisiae*, some residues of this area are contributing to enzyme activity by aiding substrate binding, see 12,13), and, 3) a region at the solvent-exposed side of TRMT112, opposite the METTL5 active site, which may be involved in interaction with yet to be identified TRMT112 partners.

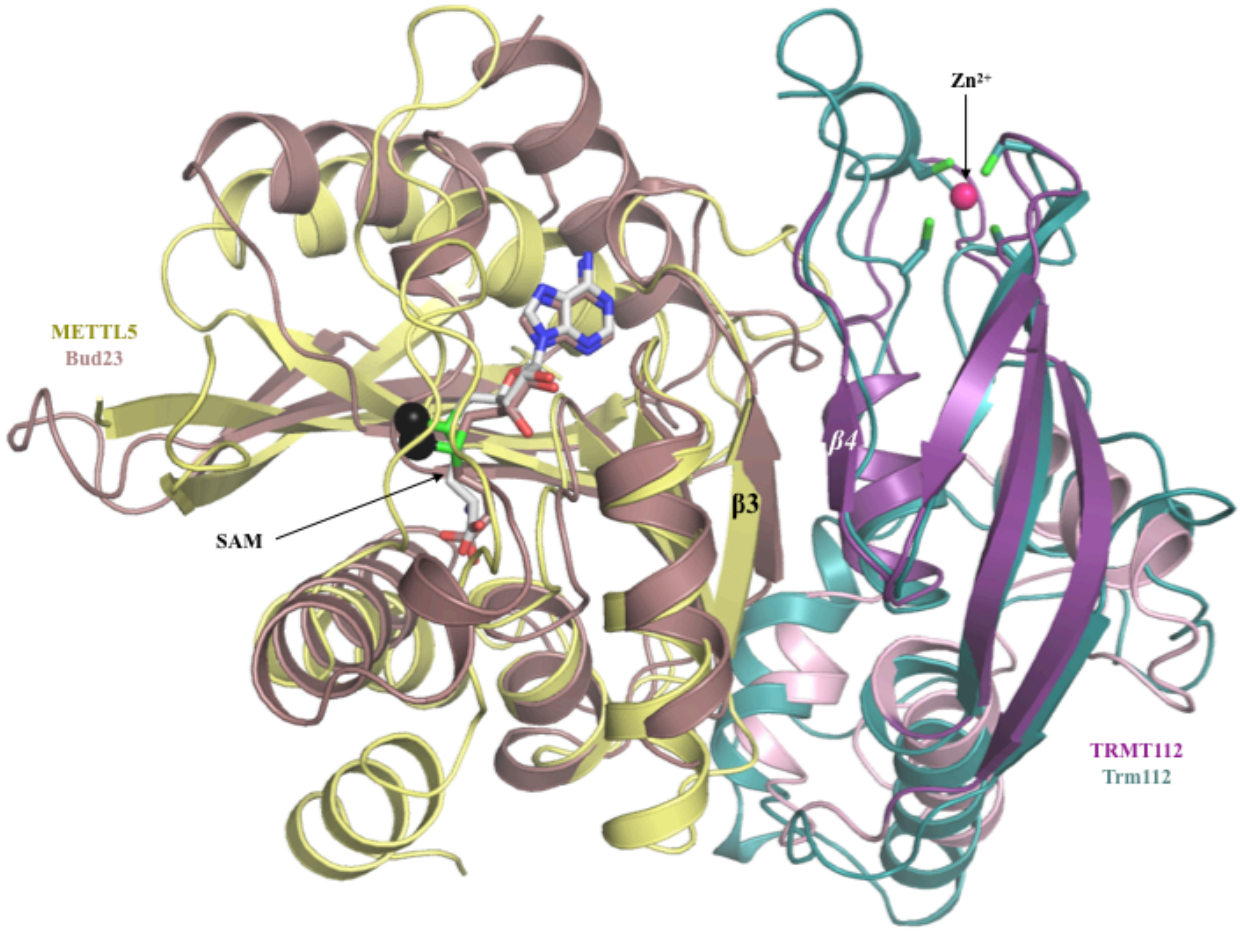

Figure S7: Superimposition of the crystal structures of human METTL5-TRMT112 and *S. cerevisiae* Bud23-Trm112 complexes

The cysteine residues involved in coordination of a zinc ion in *S. cerevisiae* Trm112 protein are shown as sticks (pointing towards the Zn^{2+}); notably, these are absent from human TRMT112, which does not bind zinc (see main text for details). The zinc ion is depicted as a magenta sphere. For the sake of clarity, only the two β-strands involved in formation of the β-zipper are labeled (β3 and β4). The SAM molecules bound to the METTL5 (gold) and Bud23 (dark salmon) methyltransferase domains are shown as sticks, with the methyl group to be transferred onto the RNA substrate (a guanosine for Bud23 and an adenosine for METTL5) shown as black spheres.

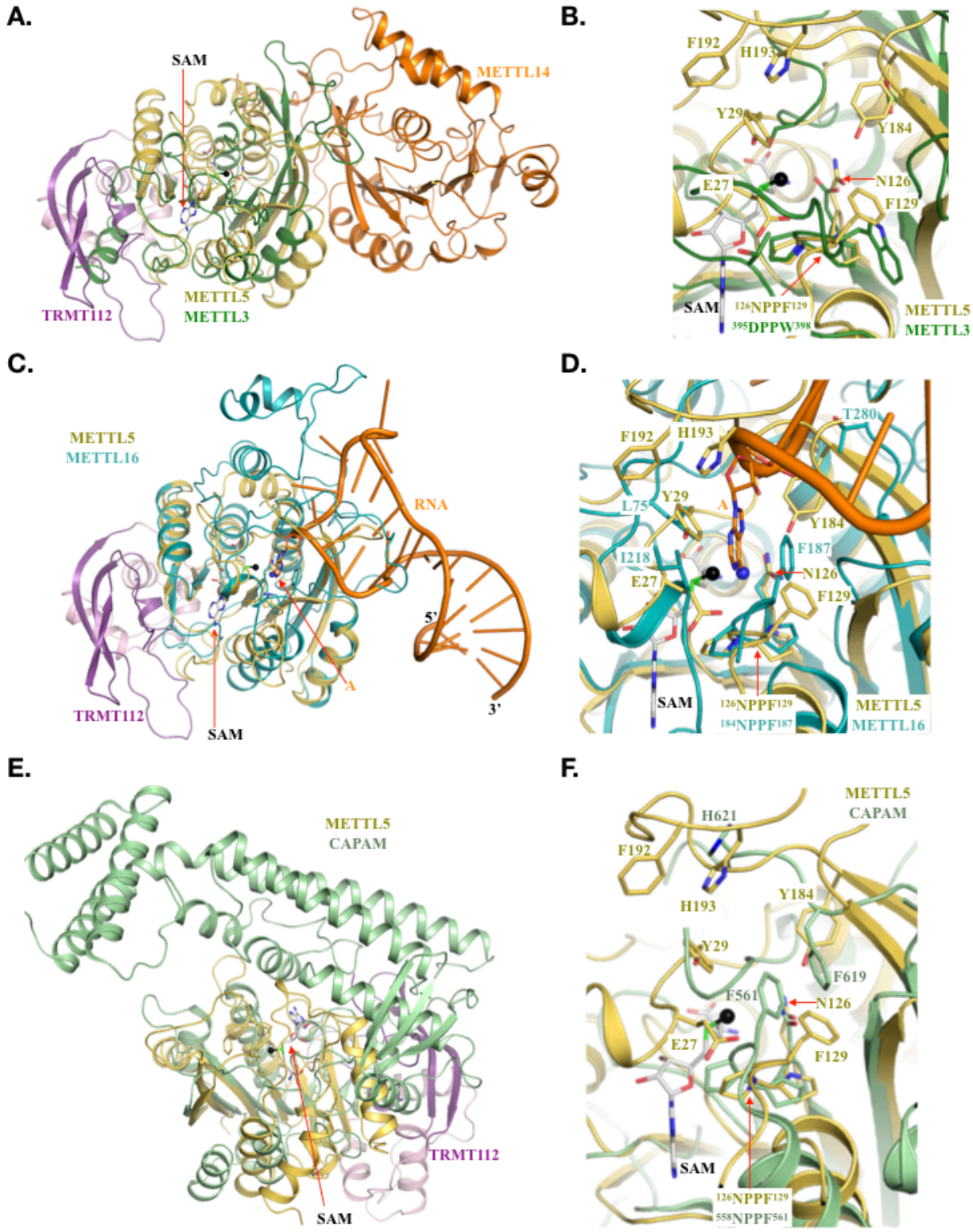

Figure S8: Comparison of the crystal structures of the human 18S rRNA (METTL5-TRMT112), mRNA (METTL3-METTL14), U6 snRNA (METTL16), and mRNA cap (CAPAM) m^{6}A methyltransferases

A. Superimposition of METTL5-TRMT112 and the METTL3-METTL14 m^{6}A mRNA methyltransferase (PDB code: 5IL1). In all panels, the SAM molecule bound to METTL5-TRMT112 complex is shown in gray sticks, and the methyl group to be transferred is depicted as a black sphere.

B. Zoom-in on the comparison between the active sites of METTL3 and METTL5. For the sake of clarity, and with the exception of the [N/D]PP[F/W], only METTL5 residues are labeled.
C. Superimposition of METTL5-TRMT112 and the METTL16 m^6A U6 snRNA methyltransferase bound to an RNA hairpin (PDB code: 6DU4). The RNA adenine (A) base modified by METTL16 is shown as orange sticks and the N6 atom, which is methylated, is shown as a blue sphere in panels C and D.
D. Zoom-in on the comparison between the active sites of METTL16 and METTL5.
E. Superimposition of METTL5-TRMT112 and the CAPAM m^6A mRNA cap-methyltransferase (PDB code: 6IRZ).
F. Zoom-in on the comparison between the active sites of CAPAM and METTL5.

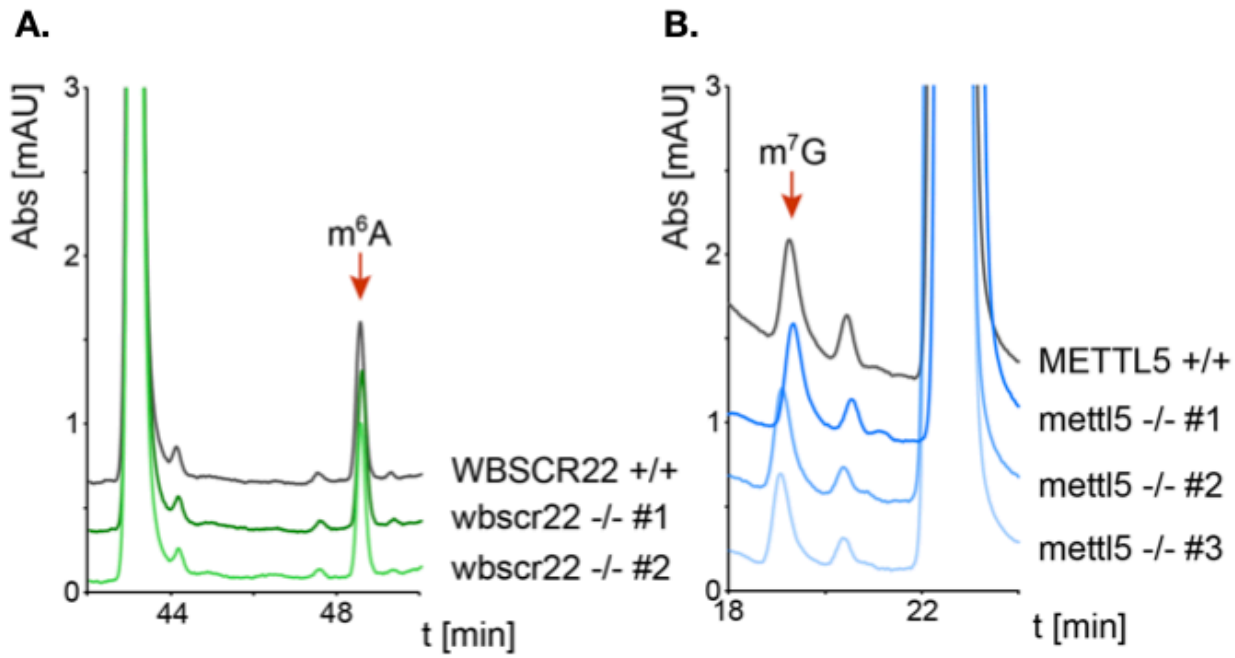

Figure S9: The m^7G_{1636} and m^6A_{1832} 18S rRNA modifications are independent of one another

A. 18S rRNA purified from two independently isolated *wbscr22* -/- cell lines and from the isogenic control (WBSCR22 +/+) was digested to single nucleotide and analyzed by HPLC. The m^6A peak, which eluates ~48.2 min, is unchanged in the mutants.
B. 18S rRNA purified from three independently isolated *mettl5* -/- cell lines and from the isogenic control (METTL5 +/+) was digested to single nucleotide and analyzed by HPLC. The m^7G peak, which eluates ~19 min, is unchanged in the mutants.

Table S1: Sequence of CRISPR-Cas9 guides and siRNAs

Gene	Name	Sequence
METTL5	crDL035	GTAACAAGAATCGGGTATAT
METTL5	crDL036	TGACATAGATGAAGACGCAT
ZCCHC4	crDL031	TGCATACTTCAAGGGCAGTC
ZCCHC4	crDL032	CAGTAATAAATTATACACCT
TRMT112	LD068	GGCCGGUUGAGGGAUAUGAtt

Table S2: Oligonucleotides used for diagnostic PCR of CRISPR-Cas9 clones

Region	Name	Sequence
METTL5-Fwd	LD4333	ATTCCTGGCCCCAAATGATC
METTL5-Rev	LD4334	GGAGCTATAAGTCGCCACTC
ZCCHC4-Fwd	LD4313	TCTGATTCACTGAGCTCAGC
ZCCHC4-Rev	LD4314	ATAGGAGCAAAGAGAGGCTTC

Table S3: Sequence of genomic DNA junctions after CRISPR-Cas9-mediated deletion of a conserved signature in the methyltransferase domain of METTL5 and ZCCHC4

For METTL5, the genomic area sequenced corresponds to chromosome 2, from position 169,821,050 to 169,821,260. For ZCCHC4, it is chromosome 4 from position 25,349,460 to 25,349,680. Sequencing confirmed that for all clones analyzed in this work (*mettl5*$^{-/-}$ #1, #2, and #3, and *zcchc4*$^{-/-}$ #1 and #2), the conserved signature of the methyltransferase domain had been successfully removed from both alleles (the cell line used, HCT116, is a diploid). It further indicated that for METTL5, clones #1 and #2 are homozygous, while clone #3 is heterozygous (one allele carrying a shorter deletion, as frequently observed in CRISPR-Cas9 genome editing experiments, hence the importance of establishing the exact nature of the mutation by sequencing). For ZCCHC4, clone #2 is homozygous while clone #1 is heterozygous (carrying slightly shorter deletions).

***mettl5*$^{-/-}$ #1**	allele 1	TTTTCTATAAATATACCAATA (169,821,071_169,821,241DEL) CGTCTTCATCTATGTCAAA
	allele 2	TTTTCTATAAATATACCAATA (169,821,071_169,821,241DEL) CGTCTTCATCTATGTCAAA
***mettl5*$^{-/-}$ #2**	allele 1	TTTTCTATAAATATACCAATA (169,821,071_169,821,241DEL) CGTCTTCATCTATGTCAAA
	allele 2	TTTTCTATAAATATACCAATA (169,821,071_169,821,241DEL) CGTCTTCATCTATGTCAAA
***mettl5*$^{-/-}$ #3**	allele 1	TTTTCTATAAATATACCAATA (169,821,071_169,821,241DEL) CGTCTTCATCTATGTCAAA
	allele 2	TTTTCT (169,821,056_169,821,081DEL) TGTTACAAACCTTTATTATTTTGGTCCCAAAGGGAGGATTCATAATTACTGTATCGAATGACTTGGACATTCTGTTAGATAATAAGCACACATCACATTGAACCATGTCAATATTTGTTAACTCAAACTCTTCTGCATTCCTATTAAATATTTCCAATGCGTCTTCATCTATGTCAAA
***zcchc4*$^{-/-}$ #1**	allele 1	CTAATTTAGAAATGAATTTTTATTTGTTCCAGAC (25,349,494_25,349,655DEL) TTACTGCAAAATAAATACATATCTAT
	allele 2	CTAATTTAGAAATGAATTTTTATTTGTTCCAGACTG (25,349,496_25,349,642DEL) GTGTATAATTTATTACTGCAAAATAAATACATATCTAT
***zcchc4*$^{-/-}$ #2**	allele 1	CTAATTTA (25,349,468_25,349,654DEL) TTACTGCAAAATAAATACATATCTAT
	allele 2	CTAATTTA (25,349,468_25,349,654DEL) TTACTGCAAAATAAATACATATCTAT

Table S4: Northern blot probes

Region	Name	Sequence
5'-ETS	LD1844	CGGAGGCCCAACCTCTCCGACGACAGGTCGCCAGAGGACAGCGTGTCAGC
ITS1	LD1827	CCTCGCCCTCCGGGCTCCGTTAATGATC
ITS2	LD1828	CTGCGAGGGAACCCCCAGCCGCGCA

Table S5: Oligonucleotides and plasmids used to over-express proteins in *E. coli*

***Hvo* genes (*Hvo* protein)**	**Enzyme**	**Plasmid generated**	**Name**	**Sequence**	Reference
HVO_1475 (*Hvo*_1475)	***NcoI***	pMG825 (pET28b; Kan^R)	oMG439	CCCTTG**CCATGG**CAACCAAGGCCGCGC	This study
	XhoI		oMG440	TTTTT**CTCGAGtta**ATGGTGATGGTGATGGTGCCACTCGATGCGGAACACTTCGG	
HVO_TRM112 (*Hvo*Trm112)		pMG564 (pET21a; Amp^R)			2
Human METTL5	***NdeI***	pMG832 (pET21a; Amp^R)			This study
	NotI				
Human ZCCHC4	***NdeI***	pMG837 (pET21a; Amp^R)			This study
	NotI				
Human TRMT112		pFF6 (pAC-Duet; Cam^R)			3

Table S6: Data collection, phasing and refinement statistics

Data collection		
Space group	$P2_12_12_1$	$P2_12_12_1$
Unit cell parameters	56.9Å; 70.6Å; 84.8Å; 90°; 90°; 90°	56.4Å; 105.9Å; 169.2Å; 90°; 90°; 90°
Wavelength (Å)	0.97857	0.97996
Resolution (Å)	50-1.6 (1.63-1.6)	50-2.5 (2.65-2.5)
R_{merge} (%)	6.8 (88.7)	14.4 (170.8)
I / σI	14 (2.1)	14.05 (1.06)
Completeness (%)	99.9 (99.9)	99.8 (99.0)
$CC_{1/2}$ (%)	99.8 (62.3)	99.9 (74.7)
Redundancy	6.1	13.5
Observed reflections	279014	487677
Unique reflections	45777	36060
Refinement		
Resolution (Å)	50-1.6	50-2.5
No. reflections	45704	36058
R / R_{free} (%)	18.6 / 21.5	21.3 / 24.9
Number of atoms		
Protein	2632	5061
SAM	27	54
SO_4^{2-} / Ethylene glycol / PEG	10 / 20 / 0	35 / 8 / 23
Water	320	28
B-factors (Å²)		
Protein	24	74
SAM	17.2	67.2
SO_4^{2-} / Ethylene glycol / PEG	52.6 / 42 / 0	137 / 87.2 / 92.3
Water	37.2	59.6
R.m.s deviations		
Bond lengths (Å)	0.006	0.01
Bond angles (°)	0.93	1.22

Table S7: Details of the electrostatic interactions involved in the METTL5-TRMT112 interface

METTL5	TRMT112
Hydrogen bonds	
Asn52 O	Arg44 Nh1
Asn52 Od1	Asn38 Nd2
Asp103 Od2	Thr5 Og1
Asp103 Od2	Lys2 N
Gln106 N	Pro114 O
Gln106 O	Met116 N
Arg115 Nh2	Phe21 O
Arg115 Ne2	Phe21 O
Salt bridges	
Arg115	Glu102
Asp121	Arg44

SUPPLEMENTARY INFORMATION REFERENCES

1. Sharma, S., Langhendries, J.L., Watzinger, P., Kotter, P., Entian, K.D. and Lafontaine, D.L. (2015) Yeast Kre33 and human NAT10 are conserved 18S rRNA cytosine acetyltransferases that modify tRNAs assisted by the adaptor Tan1/THUMPD1. *Nucleic acids research*, **43**, 2242-2258.
2. van Tran, N., Muller, L., Ross, R.L., Lestini, R., Letoquart, J., Ulryck, N., Limbach, P.A., de Crecy-Lagard, V., Cianferani, S. and Graille, M. (2018) Evolutionary insights into Trm112-methyltransferase holoenzymes involved in translation between archaea and eukaryotes. *Nucleic acids research*, **46**, 8483-8499.
3. Figaro, S., Scrima, N., Buckingham, R.H. and Heurgue-Hamard, V. (2008) HemK2 protein, encoded on human chromosome 21, methylates translation termination factor eRF1. *FEBS letters*, **582**, 2352-2356.
4. Zemp, I., Wandrey, F., Rao, S., Ashiono, C., Wyler, E., Montellese, C. and Kutay, U. (2014) CK1delta and CK1epsilon are components of human 40S subunit precursors required for cytoplasmic 40S maturation. *Journal of cell science*, **127**, 1242-1253.
5. Linder, B., Grozhik, A.V., Olarerin-George, A.O., Meydan, C., Mason, C.E. and Jaffrey, S.R. (2015) Single-nucleotide-resolution mapping of m6A and m6Am throughout the transcriptome. *Nature methods*, **12**, 767-772.
6. Olarerin-George, A.O. and Jaffrey, S.R. (2017) MetaPlotR: a Perl/R pipeline for plotting metagenes of nucleotide modifications and other transcriptomic sites. *Bioinformatics*, **33**, 1563-1564.
7. Robert, X. and Gouet, P. (2014) Deciphering key features in protein structures with the new ENDscript server. *Nucleic acids research*, **42**, W320-324.
8. Ashkenazy, H., Erez, E., Martz, E., Pupko, T. and Ben-Tal, N. (2010) ConSurf 2010: calculating evolutionary conservation in sequence and structure of proteins and nucleic acids. *Nucleic acids research*, **38**, W529-533.
9. Jo, S., Kim, T., Iyer, V.G. and Im, W. (2008) CHARMM-GUI: a web-based graphical user interface for CHARMM. *Journal of computational chemistry*, **29**, 1859-1865.
10. Jo, S., Vargyas, M., Vasko-Szedlar, J., Roux, B. and Im, W. (2008) PBEQ-Solver for online visualization of electrostatic potential of biomolecules. *Nucleic acids research*, **36**, W270-275.
11. Bourgeois, G., Letoquart, J., van Tran, N. and Graille, M. (2017) Trm112, a Protein Activator of Methyltransferases Modifying Actors of the Eukaryotic Translational Apparatus. *Biomolecules*, **7**.
12. Liger, D., Mora, L., Lazar, N., Figaro, S., Henri, J., Scrima, N., Buckingham, R.H., van Tilbeurgh, H., Heurgue-Hamard, V. and Graille, M. (2011) Mechanism of activation of methyltransferases involved in translation by the Trm112 'hub' protein. *Nucleic acids research*, **39**, 6249-6259.
13. Bourgeois, G., Marcoux, J., Saliou, J.M., Cianferani, S. and Graille, M. (2017) Activation mode of the eukaryotic m2G10 tRNA methyltransferase Trm11 by its partner protein Trm112. *Nucleic acids research*, **45**, 1971-1982.